LA-UR- 03-0148

Approved for public release;
distribution is unlimited.

Title:	CRITICAL MASSES OF URANIUM DILUTED WITH MATRIX MATERIAL (Part 1)
Author(s):	Rene Sanchez, NIS-6 David Loaiza, NIS-6 Glenn Brunson, NIS-6 Robert Kimpland, NIS-6
Submitted to:	Will be submitted to the Nuclear Science & Engineering Journal

Los Alamos
NATIONAL LABORATORY

CRITICAL MASSES OF URANIUM DILUTED WITH MATRIX MATERIAL (Part I)

by

Rene Sanchez, David Loaiza, Glenn Brunson, and Robert Kimpland

Los Alamos National Laboratory
MS-J562
Los Alamos NM, 87544
Fax (505) 665-3657

Number of Pages 30
Number of Figure 8
Number of Tables 2

CRITICAL MASSES OF URANIUM DILUTED WITH MATRIX MATERIAL (Part I)

by

Rene Sanchez, David Loaiza, Glenn Brunson, and Robert Kimpland

ABSTRACT

Scientists at the Los Alamos National Laboratory measured the critical masses of square-prisms of highly enriched uranium diluted in various X/^{235}U with matrix material and polyethylene. The configuration cores were 22.86-cm and 45.72-cm square and were reflected with 8.13-cm-thick and 10.16-cm-thick side polyethylene reflectors, respectively. The configurations had 10.16-cm thick top and bottom polyethylene reflectors. For some configurations, the Rossi-α, which is an eigenvalue characteristic for a particular configuration, was measured to establish a reactivity scale based on the degree of subcriticality. Finally, the critical mass experiments are compared with values calculated with MCNP and ENDF/B-V and ENDF/B-VI cross-section data. For the most part, the computational values agreed quite well with the experiments.

INTRODUCTION

Fissile material in waste is frequently encountered in decontamination and decommissioning activities. This radioactive waste is for the most part placed in containers or drums and stored in storage facilities throughout the Department of Energy (DOE) complex. The amount of fissile material in each drum is generally small[1] because of criticality safety limits that have been calculated with computer transport codes such as MCNP,[2] KENO,[3] or ONEDANT.[4] To the best of our knowledge, few critical mass experiments have been performed to assure the correctness of these calculations or any calculations for systems containing fissile material (^{235}U, ^{239}Pu, ^{233}U) in contact with matrix material such as Al_2O_3, CaO, MgO, SiO_2, Gd, or Fe. The experimental results presented in this paper establish the critical masses of highly enriched uranium foils diluted in various $X/^{235}U$ ratios with matrix material and polyethylene. The diluted uranium cores were 22.86-cm and 45.72-cm square and were reflected with 8.13-cm-thick and 10.16-cm-thick side reflectors, respectively. The top and bottom polyethylene reflectors were 10.16-cm thick. The polyethylene is used to represent water, which is one of the elements likely to be found in an underground radioactive waste storage facility thousands of years from now.[5]

The primary purpose of these experiments is to provide criticality data that will be used to validate models in support of the Yucca Mountain and Hanford Waste Storage Tank projects. In addition, the experiments described in this paper will help validate cross-section data used in computer neutron transport codes.

MATERIALS

The fissile material available consisted of highly enriched uranium (HEU) foils. The dimensions of the bare foils were approximately 22.86-cm square and 0.00762-cm thick. The foils were laminated with

thin plastic sheets to reduce the amount of airborne contamination. The total thickness of the foils, including the plastic sheets, was 0.02286-cm. Each foil weighed approximately 70-g and the isotopic composition was 93.23 wt% ^{235}U, 5.37 wt% ^{238}U, 0.26 wt% ^{236}U, and 1.13 wt% ^{234}U.

The diluent materials consisted of SiO_2 plates, high-density polyethylene plate inserts, 6061 aluminum plates, MgO powder, Gd foils, and Fe plates. Two types of moderating high-density polyethylene were used.

For the first series of experiments, the high-density polyethylene plates were 39.12-cm square and 1.91-cm thick. Each polyethylene plate used in the core region had a square central recess. The dimensions of the central recess were 22.86-cm square by 0.64-cm deep. The central recess was used to accommodate the SiO_2, or aluminum plates, or MgO powder, or polyethylene inserts. The dimensions of the SiO_2 plates, polyethylene inserts, and aluminum plates were approximately 22.86-cm square by 0.64-cm thick.

Because the MgO is a powdery substance that can absorb moisture from the atmosphere, each polyethylene plate containing the MgO was heated tens of degrees above room temperature so that the MgO could release this moisture. The density of the MgO was determined by weighing the empty polyethylene plate and then weighing the polyethylene plate with the MgO in the recess. The density of the MgO in each plate was calculated by dividing the weight difference between the empty and filled polyethylene plate by the recess volume. This density was then input into the MCNP model.

Because Gd has a very large absorption cross section at thermal energies, the Gd foils selected for these experiments were very small. Their dimensions were 5.08-cm square by 0.041-cm thick for one type of experiment. In order to study the effect of thickness of the Gd foil on the critical mass, thinner Gd foils were used in the second type of experiments. Their dimensions were 5.08-cm square by 0.02-cm thick. The Gd foils were placed on the center of the uranium foils. These experiments were performed with polyethylene inserts in the recesses of the moderating plates.

The low-carbon steel plates, which are mostly Fe, were 22.86-cm square by 0.038-cm thick. These plates were placed on moderating plates containing the polyethylene inserts and followed by the HEU foils.

There were eight plates that form the top and bottom reflectors (four at the top and four the bottom). Their dimensions were approximately 39.12-cm square by 2.54-cm thick.

For the second series of experiments, the high-density polyethylene plates were of two different sizes. The ones used on the bottom part of the core were 66.04-cm square by 1.05-cm thick. The ones used on the top part of the core were 75.18-cm square by 1.05-cm thick. Both types of plates had a central recess where matrix material could be accommodated. The dimensions of the central recess were 45.72-cm square by 0.64-cm deep. Four plates of matrix material (SiO_2, Al, polyethylene inserts, etc.) were needed to completely fill the central recess. The dimensions of the low-carbon steel plates used with this type of moderating plates were 45.72-cm square by 0.038-cm thick.

The experiments performed with this type of moderating plates were the 5.08-cm square by 0.041-cm thick Gd foils with polyethylene inserts in the moderating plates. The Gd foils were place on each of the

four HEU foils and interspersed between moderating plates. Other experiments included the SiO_2, and Al inserts in the moderating plates as well as the low-carbon steel plates with the polyethylene inserts in the moderating plates.

Eight polyethylene plates (four on the top and four on the bottom) form the top and bottom reflectors. Their dimensions were 66.04-cm square by 2.54-cm thick.

For all the materials, chemical analyses were performed to determine the level of impurities. In some cases, the vendors provided this information.

DESCRIPTION OF EXPERIMENTS

The experiments were performed on the Planet general-purpose vertical machine shown in Fig. 1. This machine consists of a hydraulic lift directly beneath a stationary aluminum platform, which lifts the bottom part of the experiment that rests on a movable platen approximately 22–30 cm. Four jackscrews driven very precisely by a stepping motor move the platen the final 4.5-cm of separation. Figure 1 shows the setup for the measurements of the HEU foils-SiO_2-polyethylene experiment. For the final approach to critical, typically half of the critical mass is placed on the top platform and the other half is placed on the movable platen.

As seen in Fig. 1, there is a hollow aluminum cylinder and a 10 kg weight on the top reflector. The weight is there to ensure that there is full compression of the stack. Because most of the experiments were not infinitely reflected systems, a hollow cylinder was used to separate the 10 kg from the top of

the reflector. This action minimizes the number of neutrons reflected from the 10 kg weight back into the system. Therefore, the reactivity worth of the 10 kg weight can be assumed to be zero and independent of its position on the top of the reflector.

Figure 2 shows a cross-section view of the experiments and their approximate final configuration. Note that the laminated HEU foils are in direct contact with the matrix material. Figure 3 and 4 show the different types of experiments performed with matrix materials.

The starting configuration for all experiments contained less than 800 g HEU, which is approximately the minimum critical mass for a homogeneous water-moderated, water-reflected HEU sphere. A 1/M approach to critical was performed following the guidelines of the existing operating procedures.

The starting configuration also contained a Pu-Be neutron source to enhance the neutrons that leak out of the system. The neutron leakage from the hand-stacking assembly was measured with four BF_3 neutron detectors. The total number of counts in a 100-seccond time interval was normalized and plotted as unity on a graph of counting rate ratios versus number of unit cells. The next unit was added and once again the neutron leakage measured. The new total number of counts in a 100-second time interval was divided by the total number of counts obtained in the previous step. The reciprocal of this number was plotted again on the same graph of counting ratios versus number of unit cells. A line that passed through the two points was extrapolated to the x-axis, which represented the number of unit cells, to obtain the extrapolated critical number of units.

Once the extrapolated critical number of units was obtained, two guidelines or rules were observed before adding any more fissile material into the hand-stacking assembly. The first rule was the 75% rule, which simply states that hand-stacking operations should continue until the next addition of fissile material exceeds 75% of the extrapolated critical mass. The second rule was the halfway rule, which states that hand-stacking operations should continue as long as the individual steps taken (addition of fissile material, control rod position, separation distance between two stacks, etc.) do not double the multiplication of the system or the count rate. This rule is based on the assumption that there is a linear relationship between the multiplication of the system and the changing parameter (addition of fuel, gap distance, etc.).

Once the hand-stacking limit was reached, the experiment was split into two parts. The bottom part of the core, which contained approximately half of the critical mass, was placed on the movable platen of the Planet assembly. The top part of the core was placed on the top platform of the Planet assembly and typically contained two or three unit cells, which represented 5% to 10% of the critical mass.

The movable platen, which contained the Pu-Be neutron source, was then raised remotely until it contacted the top portion of the stack. The neutron leakage from the assembly was measured with the same four BF_3 neutron detectors used during the hand-stacking operation. Because the position of the neutron detectors changed with respect to the neutron detectors of the earlier hand-stacking operation, the total number of counts in a 100-second time interval was renormalized and plotted as a unity on a graph of counting rate ratios versus number of unit cells. After disassembly, uranium foils, diluent materials, and polyethylene plates were added to the top of the stack observing only the halfway rule. The movable platen was raised one more time until both portions of the stack were in direct contact with each other

and the neutron leakage was again measured. The total number of counts in a 100-second time interval was divided by the total number of counts obtained in the previous step and its reciprocal plotted on the same graph to obtain an extrapolated critical number of units. This operation continued until a high multiplication was attained (Fig. 5). For the last units, a 1/M as a function of separation (Fig. 6) was performed to attain the critical separation or the excess reactivity of the system.

ROSSI-α MEASUREMENTS

The purpose of the Rossi-α measurements was to establish the degree of subcriticality as a function of the separation between top and bottom parts of the core. The Rossi-α technique[6] correlates time decay constants for the prompt–neutron-linked fission chains with reactivity. The prompt neutron decay constants at delayed critical represent an eigenvalue characteristic of these particular configurations, which can be calculated by a deterministic or Monte Carlo neutron transport method.

The Rossi-α measurements were performed on three configurations. One of these configurations contained HEU foils diluted with (1×1) Al plates and polyethylene arranged as shown in Fig. 2. For the second configuration, the Al plates were substituted with (1×1) SiO_2 and arranged similarly, as illustrated in Fig. 2. For both configurations, one of the polyethylene plates located in the center of the assembly had holes drilled in the radial direction that were used to accommodate highly sensitive ^3He neutron detectors. The third configuration contained (2 × 2) HEU foils on the top of thin low-carbon steel plates sandwiched between moderating polyethylene plates. For this configuration, the ^3He neutron detectors were placed on the top of the bottom part of the core.

The data were collected with a time analyzer that had the capability of time tagging each arrival pulse from each of the neutron detectors and sorting them one by one into time bins according to their time of arrival. For the first two experiments, the time analyzer operated in the auto-correlation mode and cross-correlation mode for last experiment. The stored data could be analyzed using different time widths without having to retake the data. The alphas to both experiments at different subcritical separations were obtained from the least square fits to the forms

$$F(t)=A\exp(-\alpha t) + C \qquad (1)$$

$$F(t)= A\exp(-\alpha_1 t) + B\exp(-\alpha_2 t) + C. \qquad (2)$$

The prompt neutron decay constants at delayed critical were obtained by plotting the alphas at a particular subcritical separation as a function of the inverse count rate and extrapolating linearly to an inverse count rate of zero (delayed critical).

Knowing that α is zero at prompt critical, a linear relationship was established between α and the degree of subcriticality (see Fig. 7). For the $^{235}U/SiO_2$/polyethylene experiment, this relationship is

$$\alpha = (2.231 \pm 0.04)\,(100 - \rho)\ \text{sec}^{-1}, \qquad (3)$$

where ρ is the reactivity of the system in cents and α is the prompt neutron decay constant in 1/sec. A similar expression was established for the ^{235}U/Al/polyethylene experiment. For the ^{235}U/Fe/polyethylene experiment, this relationship is

$$\alpha = (3.02 \pm 0.03)\,(100 - \rho)\ \text{sec}^{-1}, \qquad (4)$$

Table I shows the delayed critical prompt neutron decay constants for both experiments. It is important to note that for both experiments the least square fit to "one exponential function (Eq. 1)" was not the perfect fit. Several reasons can explain this behavior. One is that the systems were operated at high mul-

tiplications (high fission rates), which caused overlapping of longer fission chains. Another reason is that the uncorrelated (background) constant, which is represented by C in Eqs. 1 and 2, increases as the square of the power level and the correlated term (signal) increases proportional to the power. Therefore, the signal-to-background ratio decreases more rapidly as the power level increases, which causes some of the information in the exponential term to be lost and possibly affects the one exponential fit. Nonetheless, when the neutron source was removed from the system and the measurements were performed for longer periods of time at these high multiplications, the fit approached a "one exponential" function. In addition, for the two exponential function (Eq. 2), the ratio of the amplitude, A, of the fundamental mode exponential to the second exponential amplitude, B, tends to increase as the configuration approaches delayed critical. This indicates that the second exponential tends to diminish as the system approaches the fundamental mode and the decay constant, α_1, of the fundamental mode exponential in Eq. 2 approaches the one for the one exponential fit (see Table I).

For the third experiment, the system operated at relative lower multiplications compared with the first two experiments. It was found that a one exponential fit was quite adequate to represent the experimental data. Because this system contains less polyethylene than the first two experiments, the alpha at delayed critical is slightly larger (see Table I), which indicates a harder neutron spectrum.

It is interesting to point out that the alphas at delayed critical for the first two experiments are statistically the same, which indicates that the neutron lifetime is approximately the same for both systems. Calculations performed with MCNP yielded a β_{eff} of 0.0068 for the $^{235}U/SiO_2$/polyethylene experiment and 0.00692 for the ^{235}U/Al/polyethylene experiment. At delayed critical, $\alpha_{dc}=\beta_{eff}/l$ where l is the prompt neutron lifetime. Thus, the neutron lifetime for these systems is on the order of 30 μs. Finally, the tem-

perature of the experiments was kept within ± 1°C for each run at a particular separation, which meant that the reactivity or multiplication of the system did not change significantly, considering that the reactivity temperature coefficient for these experiments was –$0.003/°C.

RESULTS

Table II summarizes the critical masses obtained for the different configurations as well as the calculated k_{eff} for each system. In some cases, it was deemed appropriate to add a bit more of the extrapolated critical mass to the system to obtain an asymptotic reactor period and in this way to determine the excess reactivity (in cents) above delayed critical through the Inhour equation. An MCNP calculation was performed for each configuration to determine β_{eff} and be able to convert from reactivity in cents to absolute k.

As seen in Table II, there were two experiments (1×1) with Gd foils ($Gd/^{235}U$=0.09, $Gd/^{235}U$=0.04) that essentially had the same amount of hydrogen content $H/^{235}U$=230. These experiments investigated the optimal thickness of the 5.08-cm square Gd foil that would yield the greatest increase in the critical mass. As seen in this table, the critical mass changes from 1301 g with no Gd ($H/^{235}U$=220) to 1893 g with the thin Gd foils and 1958 g with the thicker ones. Based on the results of these experiments, the thicker Gd foils (111 g) do not make a significant difference in the critical mass when compared with the critical mass obtained with thinner Gd foils (56 g). Therefore, the thinner Gd foils may be already 90% black to neutrons and increasing the thickness of these foils is not going to significantly increase the critical mass.

In the other experiment (2 × 2) with Gd foils (337 g) and polyethylene ($Gd/^{235}U$=0.18, $H/^{235}U$=245), the critical mass increases slightly when compared with a similar experiment with no Gd ($H/^{235}U$=239). This is due to the fact that the neutron absorption cross-section for Gd exhibits a 1/v behavior and the Gd is less effective as a neutron absorber in a harder neutron spectrum. Figure 8 shows the normalized flux obtained with MCNP in the center region for two Gd experiments. As seen in this figure, the 45.72-cm square core ($Gd/^{235}U$=0.18, $H/^{235}U$=245) experiment has a harder spectrum than the 22.86-cm square core ($Gd/^{235}U$=0.09, $H/^{235}U$=230) experiment even though the hydrogen to uranium ratio of the first experiment appears to be greater than the second experiment. Another important point is that the unit cell in the second ($Gd/^{235}U$=0.09, $H/^{235}U$=230) experiment consists of a Gd foil on the top of two uranium foils followed by the moderating polyethylene plate. Because the fuel is not homogenously distributed throughout the core, some shelf-shielding of the fuel may be occurring and the true $H/^{235}U$ ratio may be higher than 230. This would explain why the second experiment with lower $H/^{235}U$ ratio is more thermal than the first one and why Gd is more effective as a neutron absorber in the second experiment compared with the first one.

Three experiments were performed with SiO_2 and polyethylene. For the (1×1) $Si/^{235}U$= 42 and $H/^{235}U$ =312 experiment, the configuration is approaching an infinite cylinder and it may never attain criticality. An MCNP calculation of this experiment, including gaps and lamination of the HEU foils, yielded a k_{eff} of 0.98. Adding more fuel and moderating materials to the MCNP model caused the k_{eff} to increase and level at 0.99. The other two SiO_2 experiments investigated the effect on the critical mass of reducing the amount of hydrogen and increasing the amount of glass in the experiments. As seen in Table II, the critical mass for (1×1) $Si/^{235}U$=21, $H/^{235}U$=156 is 2285.3 g and increases to 6456.3 g for (2 × 2) $Si/^{235}U$=42.7, $H/^{235}U$=105. The difference in the critical mass is due entirely to the difference in the

moderation for both systems. Although there is more SiO_2 (64-kg) in the 2 × 2 experiment than in the 1×1 (11-kg), glass is not as good moderator as polyethylene and this is why the critical mass increased for the 2 × 2 experiment. Similar experiments were performed with aluminum and low-carbon steel plates. Both aluminum and iron are again not very good moderators and in both cases the critical masses for both systems increase as the hydrogen is reduced.

In two cases ($H/^{235}U = 220$, and $H/^{235}U = 239$), the bottom part of the core was never in direct contact with the top part of the core because the estimated excess reactivity exceeded \$0.50 above delayed critical when fully closed. To determine precisely the excess reactivity when the two halves were together, several reactors periods were obtained as a function of separation and converted into reactivity through the Inhour equation. A plot of reactivity as a function of separation was generated, and based on a linear relationship the excess reactivity was estimated when the system was fully closed. This excess reactivity in cents was converted to absolute k using Eq. 5. The new k_{eff} was then input into the last column of Table II as the experimental k_{eff}.

$$\rho(\$) = \frac{k_{eff} - 1}{k_{eff} * \beta_{eff}} \qquad (5)$$

For all other experiments where the reported experimental k_{eff} is greater than one, both halves were in direct contact and an exponential rise in the neutron population was observed. The reactor periods obtained from the raising neutron population were again converted to reactivity through the Inhour equation. The resulting reactivity was always less than 50 cents. The excess reactivity was converted to absolute k again using Eq. 5.

For those experiments where the experimental k_{eff} is reported as less than 1 in Table III, the k_{eff} was estimated by the following formula

$$k_{eff} = (M/M_{ec})^{1/3}, \qquad (6)$$

where M is the uranium mass in the experiment and M_{ec} is the extrapolated critical mass from the 1/M plot. This relationship[7] is extremely accurate, especially when the multiplication of the system is above 100. It is important to mention that the reproducibility of all the experiments, that is taking the experiment apart and putting it back together, was ± 3 cents.

The MCNP-4C transport computer code was used to estimate the k_{eff} for each system. For most of the cases, a total of three million histories were run. The code was operated in the k-code mode using continuous energy cross-sections based on ENDF/B-V and VI. The MCNP calculations were performed using cross-section and $S(\alpha,\beta)$ data at room temperature.

For the most part, the calculated values agreed quite well with the experimental k_{eff}. The exception is in the experiment that contains MgO. The calculated k_{eff} is approximately 4% higher than the experimental value and it is independent of the type of cross section used. Souto[8] and others are presently investigating this discrepancy. However, it is believed that impurities in the MgO, which were not considered in the calculations, may be the cause for this discrepancy.

CONCLUSIONS

Several experiments were performed at the Los Alamos Critical Experiments Facility to measure the critical mass of HEU diluted with matrix materials. For some experiments, Rossi-α measurements were performed to establish a scale of reactivity. These experiments were modeled with MCNP and, for the

most part, the calculated k_{eff} agreed quite well with the experimental values. However, for the MgO experiment, a discrepancy of 4% was found between calculation and experiment. This discrepancy is being investigated.

ACKNOWLEDGMENTS

The authors would like to acknowledge Charlene Cappiello and her operating staff for providing the mechanical engineering support needed for these experiments. We also would like to thank the operating staff of the Los Alamos Critical Experiments Facility for their help during the operation of the experiments.

REFERENCES

1. M. E Shaw, J. Blair Briggs, et al., "Criticality Safety Evaluation for TRU Waste in Storage at RWMC," Idaho National Engineering Laboratory report EGG-NRE-10754, (1994).

2. J. F. Briesmeister, "MCNP-A General Monte Carlo N-Particle Transport Code," Los Alamos National Laboratory report LA-12625-M, Version 4C, (March 2000).

3. D. F. Hollenback, L. M. Petrie, and N. F. Landers, "KENO-IV: A General Quadratic Version of the KENO Program," Oak Ridge National Laboratory report ORNL/NUREG/CDS-2/V2/R6.

4. R. D. O'Dell, F. W. Brinkley, Jr., and D. R. Marr, "User's Manual for ONEDANT: A Code Package for One-Dimensional, Diffusion-Accelerated, Neutral-Particle Transport," Los Alamos National Laboratory report LA-9184-M (1982).

5. B. F. Gore, U. P. Jenquin, and R. J. Serne, "Factors Affecting Criticality for Spent-Fuel Materials in a Geologic Setting," PNL-3791, Pacific Northwest Laboratory.

6. J. Orndoff, "Prompt Neutron Periods of Metal Critical Assemblies," *Nucl. Sci. & Eng.*, 2, 450, (1957).

7. D. O'Dell, "k_{eff} vs Fraction of Critical Mass," Los Alamos National Laboratory Memorandum, ESH-6-96-092, Los Alamos, New Mexico (June 1996).

8. F. Souto and D. Loaiza, "Analysis of the Discrepancy Between the Measured and Calculated keff for the HEU-MgO Criticality Experiment at the Planet Universal Assembly," ANS Transactions, Vol. 87, 381, (2002).

9. R. Brewer and R. Sanchez, "HEU-SiO_2-Polyethylene-Reflected Critical Assembly," ANS Transactions, Vol. 84, 282, (2001).

10. D. Loaiza and R. Sanchez, "Benchmark Calculations for the Diluted Highly Enriched (HEU) and Aluminum Experiment," ANS Transactions, Vol. 85, 157, (2001).

11. D. Loaiza and R. Sanchez, "Benchmark Analysis for the HEU-Fe Critical Experiment," ANS Transactions, Vol. 87, 383, (2002).

12. D. Loaiza, Los Alamos National Laboratory, personal communications, (December 2002).

Title: The HEU waste matrix experiment mounted on the Planet assembly.

Authors: Rene Sanchez, David Loaiza, Glenn Brunson, and Robert Kimpland.

Figure: #1

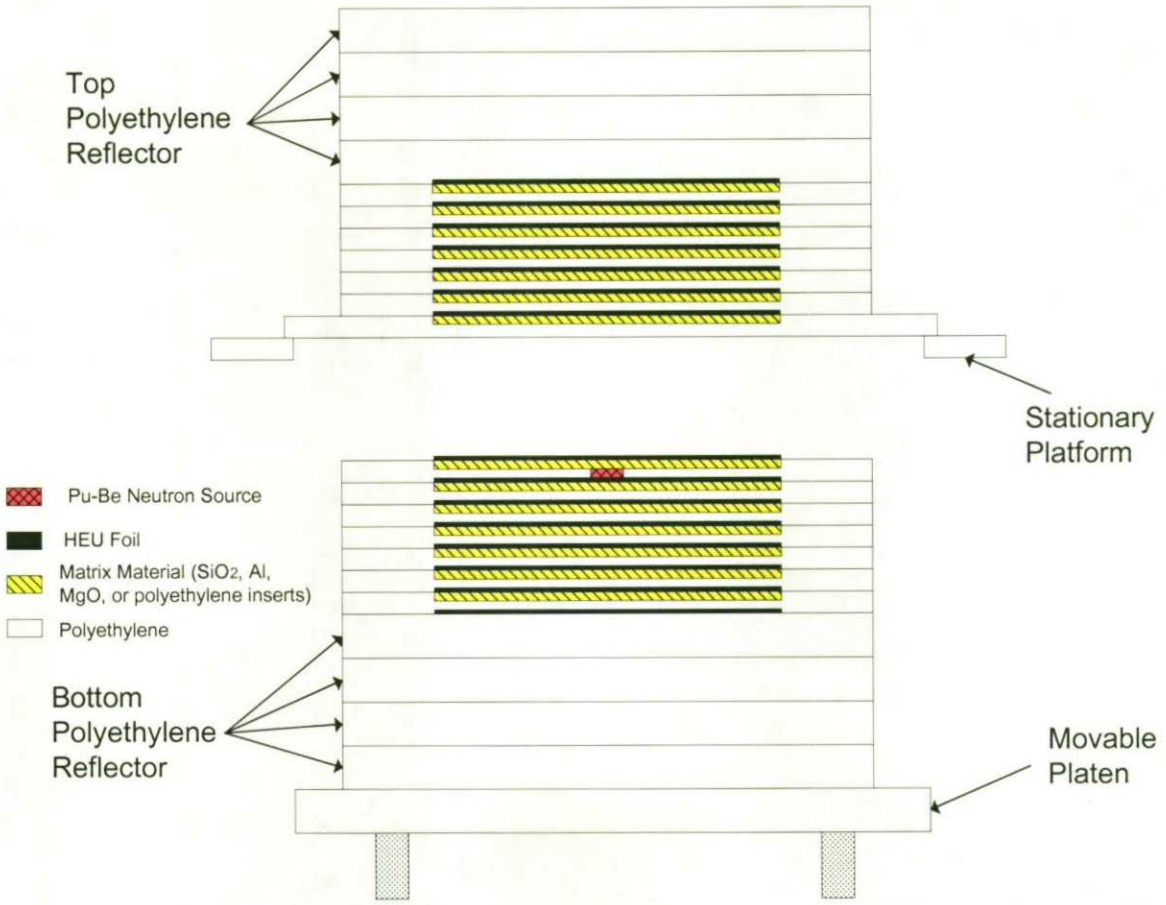

Title: Approximate final configuration for the diluted HEU experiments.

Authors: Rene Sanchez, David Loaiza, Glenn Brunson, and Robert Kimpland.

Figure: #2

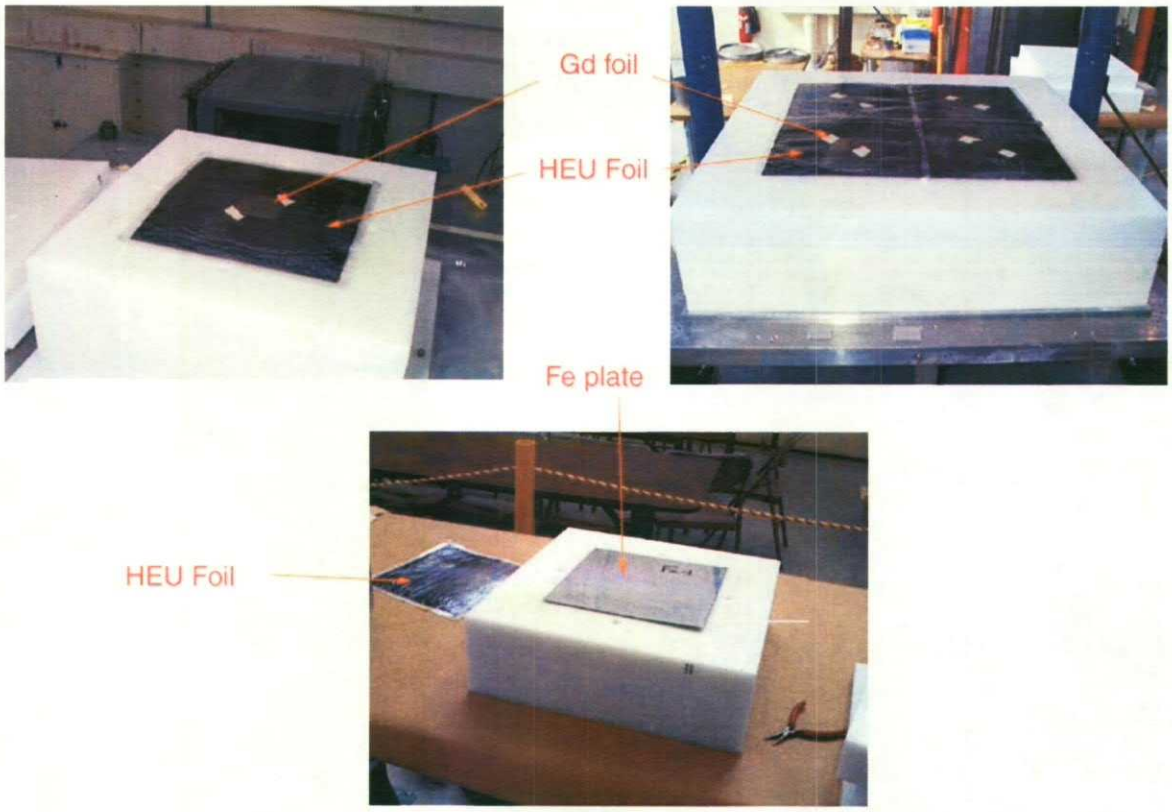

Title: Gadolinium and iron critical-mass experiments.

Authors: Rene Sanchez, David Loaiza, Glenn Brunson, and Robert Kimpland.

Figure: #3

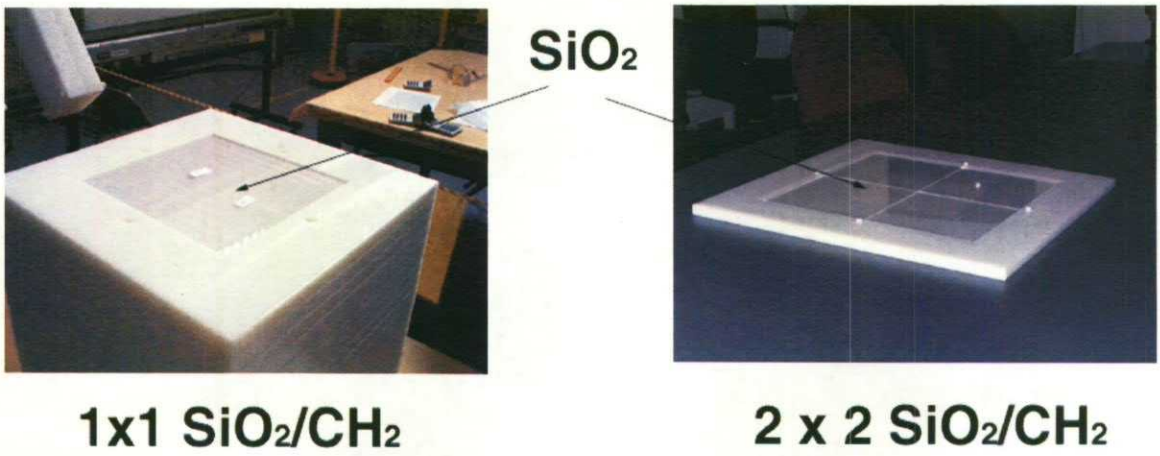

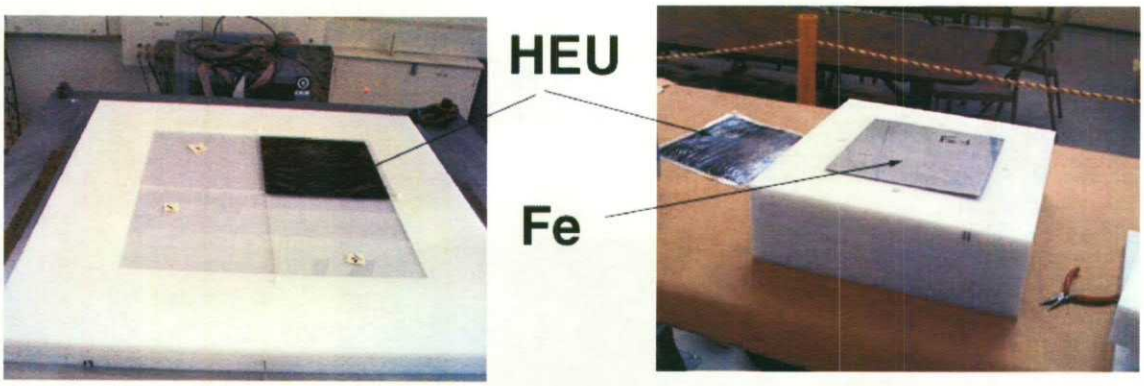

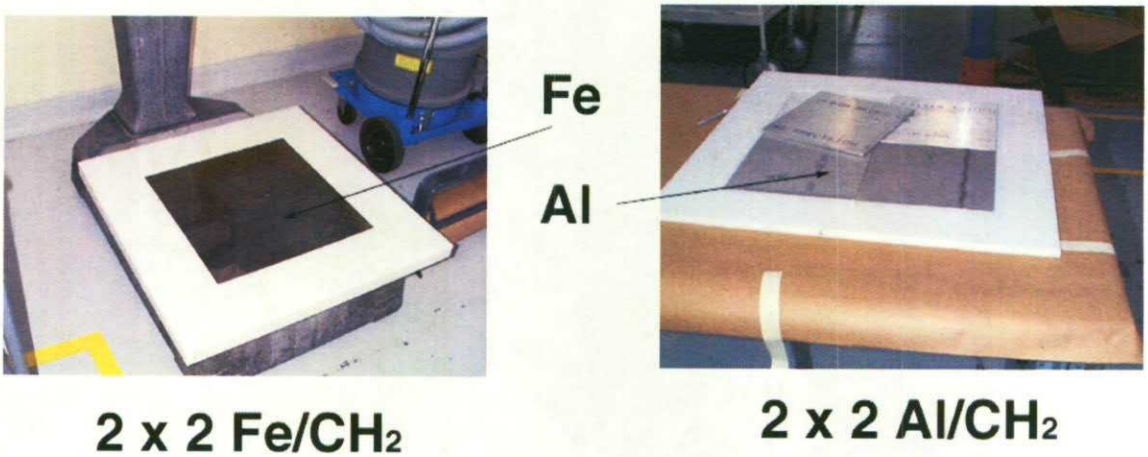

Title: Other matrix material critical experiments.

Authors: Rene Sanchez, David Loaiza, Glenn Brunson, and Robert Kimpland.

Figure: #4

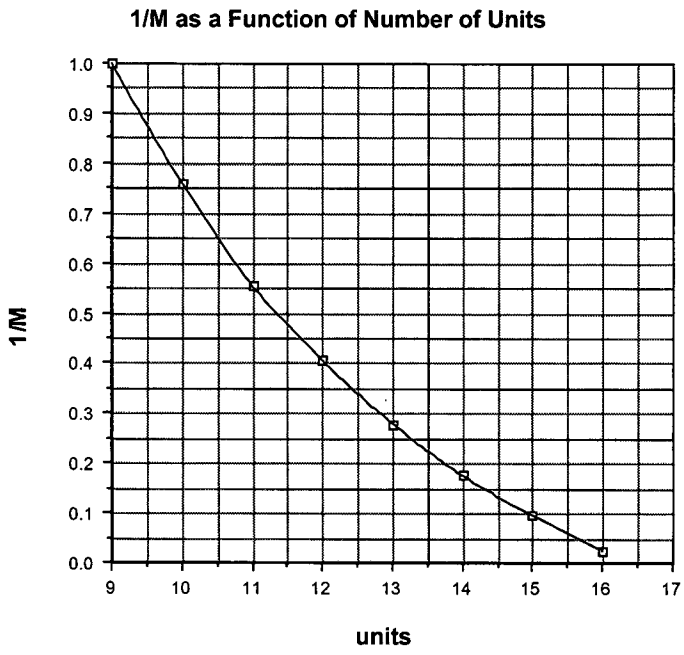

Title: Normalized 1/M as a function of highly enriched HEU foils for ^{235}U-SiO_2-polyethylene experiment. Two HEU foils represent a unit.

Authors: Rene Sanchez, David Loaiza, Glenn Brunson, and Robert Kimpland.

Figure: #5

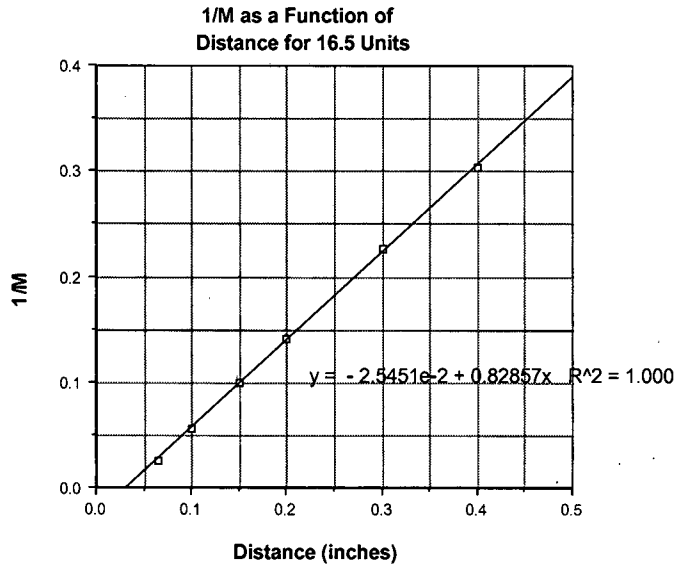

Title: Normalized 1/M as a function of separation for ^{235}U-SiO_2-polyethylene experiment.

Authors: Rene Sanchez, David Loaiza, Glenn Brunson, and Robert Kimpland.

Figure: #6

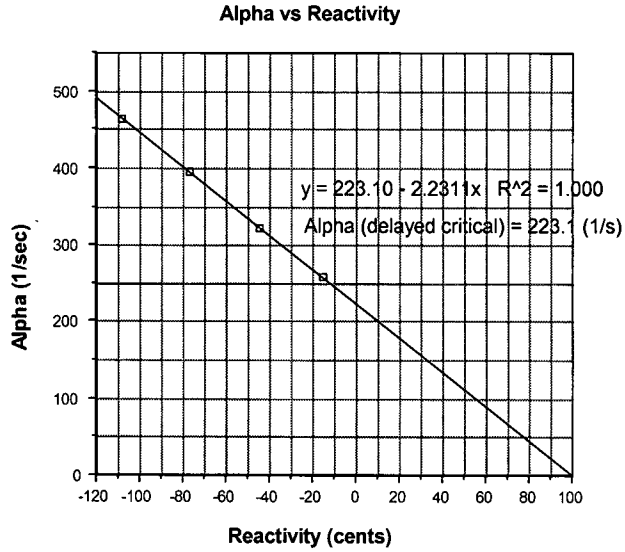

Title: Rossi-α as a function of reactivity for ^{235}U-SiO_2-polyethylene experiment.

Authors: Rene Sanchez, David Loaiza, Glenn Brunson, and Robert Kimpland.

Figure: #7

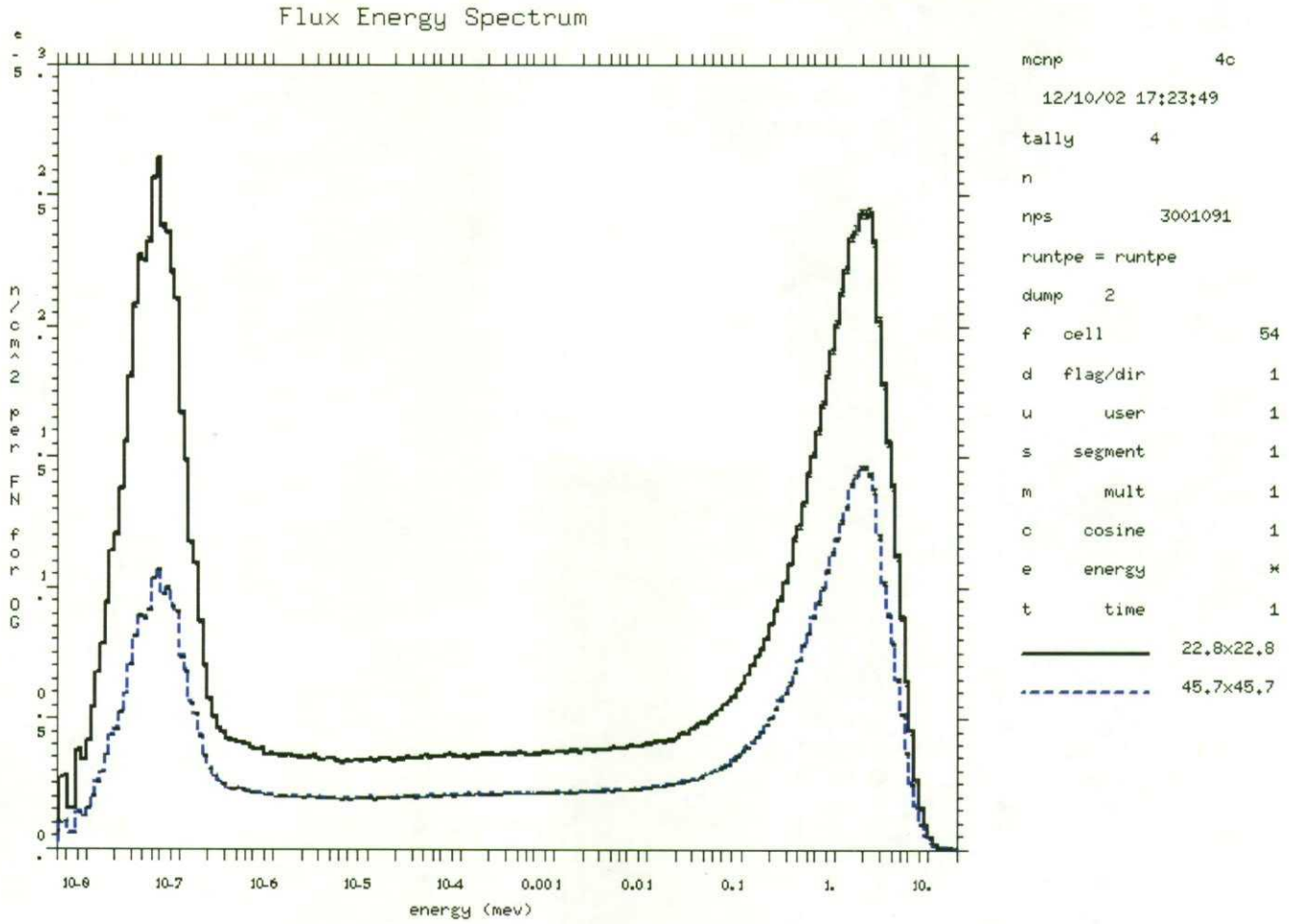

Title: Flux energy spectra in the center of the Gd/HEU/polyethylene assemblies for the two different sized core experiments.

Authors: Rene Sanchez, David Loaiza, Glenn Brunson, and Robert Kimpland.

Figure: #8

Table I.

Title: Prompt neutron decay constants at delayed critical for uranium diluted with matrix material systems.

Authors: Rene Sanchez, David Loaiza, Glenn Brunson, and Robert Kimpland.

Uranium/SiO_2/Polyethylene. $Si/^{235}U = 21$, $H/^{235}U = 156$. Detector and source locations	α(1/s) at delayed critical (DC)		Temperature (°C)
Detectors were placed in the center of the assembly approximately 18.4-cm from the top reflector. Neutron source was placed on the movable platen.	223.1 ± 4.0		25.5
	α_1(1/s) at DC	α_2(1/s) at DC	
	218.3 ± 2.0	13500 ± 3500	
Uranium/Al/Polyethylene. $Al/^{235}U = 60$, $H/^{235}U = 159$. Detector and source locations	α(1/s) at DC		Temperature (°C)
Detectors were placed in the center of the assembly approximately 20.3-cm from the top reflector. Neutron source was placed for some runs in the movable part of the core and for other runs in the stationary part of the core.	212.8 ± 9.0		25.6
	α_1(1/s) at DC	α_2(1/s) at DC	
	209 ± 9.0	-	
Uranium/Fe/Polyethylene. $Fe/^{235}U = 9.4$, $H/^{235}U = 202$. Detector and source locations	α(1/s) at DC		Temperature (°C)
Detectors were placed on the top of the bottom part of the core. Neutron source was placed on the movable part of the core.	301.9 ± 3.0		26.8

Table II.

Title: Critical masses and parameters of uranium-diluted systems.

Authors: Rene Sanchez, David Loaiza, Glenn Brunson, and Robert Kimpland.

Final measured configuration			Critical configuration			k_{eff}
Diluent	$X/^{235}U$, $H/^{235}U$	Mass of Uranium (g)	Extrapolated critical mass g of U	Core average density (g/cc) U	Core average density (g/cc) diluent	
SiO_2/ polyethylene	$Si/^{235}U = 42$, $H/^{235}U = 312$	2196	2878	0.071	For SiO_2 density = 0.74 For CH_2 density = 0.64	
SiO_2/ polyethylene	$Si/^{235}U = 21$, $H/^{235}U = 156$	2233.1	2285.3	0.149	For SiO_2 density = 0.77 For CH_2 density = 0.66	1.002 Exp 1.0070 Cal ± 0.0015 ENDF/B-V[9]
SiO_2/ polyethylene	$Si/^{235}U = 43$, $H/^{235}U = 105$	6324.3	6456.3	0.130	For SiO_2 density = 1.32 For CH_2 density = 0.382	0.9931 Exp 1.00128 Cal ± 0.00034 ENDF/B-VI[12]
Al/ polyethylene	$Al/^{235}U = 60$, $H/^{235}U = 159$	2604.0	2609.1	0.145	For Al density = 0.93 For CH_2 density = 0.66	1.001 Exp 1.0016 Cal ± 0.0004 ENDF/B-VI[10]
Al/ Polyethylene	$Al/^{235}U = 120$, $H/^{235}U = 110$	7354.2	7572.2	0.128	For Al density = 1.68 For CH_2 density = 0.382	0.9903 Exp 0.99838 Cal ± 0.00034 ENDF/B-VI[12]
MgO/ polyethylene	$Mg/^{235}U = 18$, $H/^{235}U = 160$	2878	2950.8	0.145	For MgO density = 0.42 For CH_2 density = 0.64	1.0009 Exp 1.0435 Cal ± 0.0004 ENDF/B-VI[8]
Gd/ polyethylene	$Gd/^{235}U = 0.09$, $H/^{235}U = 230$	1951.3	1958.3	0.146	For Gd density = 0.008 For CH_2 density = 0.96	0.9976 Exp 1.00149 Cal ± 0.0005 ENDF/B-VI
Gd/ polyethylene	$Gd/^{235}U = 0.046$, $H/^{235}U = 228$	1811.0	1893.6	0.15	For Gd density = 0.004 For CH_2 density = 0.96	1.0025 Exp 1.00602 Cal ± 0.0005 ENDF/B-VI
Gd/ polyethylene	$Gd/^{235}U = 0.18$, $H/^{235}U = 245$	2801.0	2872.8	0.141	For Gd density = 0.016 For CH_2 density = 0.96	0.9905 Exp 1.00354 Cal ± 0.0005 ENDF/B-VI
Fe/ polyethylene	$Fe/^{235}U = 4.51$, $H/^{235}U = 224$	1388	1408.9	0.154	For Fe density = 0.15 For CH_2 density = 0.96	0.9973 Exp 1.0096 Cal ± 0.0003 ENDF/B-VI[11]

Fe/ polyethylene	Fe/^{235}U = 9.4, H/^{235}U = 202	2470.0	2665.9	0.140	For Fe density = 0.28 For CH_2 density = 0.96	1.00009 Exp 0.99903 Cal ± 0.00034 ENDF/B-VI[12]
Polyethylene	H/^{235}U = 220	1251.0	1301.4	0.157	For CH_2 density = 0.96	1.0050 Exp 1.0146 Cal ± 0.0005 ENDF/B-VI
Polyethylene	H/^{235}U = 471	1319.0	1331.6	0.073	For CH_2 density = 0.96	0.9969 Exp 0.9909 Cal ± 0.0004 ENDF/B-VI
Polyethylene	H/^{235}U = 239	2233.1	2454.3	0.145	For CH_2 density = 0.96	1.0079 Exp 1.0137 Cal ± 0.0005 ENDF/B-VI

Figure 1. The HEU waste matrix experiment mounted on the Planet assembly.

Figure 2. Approximate final configuration for the diluted HEU experiments.

Figure 3. Gadolinium and iron critical-mass experiments.

Figure 4. Other matrix material experiments.

Figure 5. Normalized 1/M as a function of highly enriched HEU foils for ^{235}U-SiO_2-polyethylene experiment. Two HEU foils represent a unit.

Figure 6. Normalized 1/M as a function of separation for ^{235}U-SiO_2-polyethylene experiment.

Figure 7. Rossi-α as a function of reactivity for ^{235}U-SiO_2-polyethylene experiment.

Figure 8. Flux energy spectra in the center of the Gd/HEU/polyethylene assemblies for the two different sized core experiments.